ChemPubSoc Europe

DOI: 10.1002/chem.201405469

CHEMISTRY
A European Journal
Full Paper

Boron Nitride

Chitosan-Templated Synthesis of Few-Layers Boron Nitride and its Unforeseen Activity as a Fenton Catalyst

Ana Primo,*[a] Sergio Navalón,[a] Abdullah M. Asiri,[b] and Hermenegildo García*[a, b]

Abstract: A novel procedure for the preparation of few-layers boron nitride (BN), either as films or as suspended BN platelets, is presented, based on the pyrolysis of chitosan, which serves both as a matrix to embed ammonium borate and as a template for BN synthesis. The resulting BN samples are characterized by XRD, Raman and X-ray photoelectron spectroscopy, and by TEM and AFM imaging. The samples exhibit deep UV emission, which is characteristic of high quality BN. This template synthesis and the easy exfoliation of BN platelets facilitate the use of BN as an extremely high-efficiency Fenton catalyst for the generation of highly aggressive hydroxyl radicals in water.

Introduction

Hexagonal boron nitride (h-BN) is constituted by layers of alternating boron and nitrogen atoms in hexagonal arrangement having a graphite-like structure.[1,2] Single-layer BN (sl-BN) is one atom thick two-dimensional (2D) material isostructural with graphene.[3] However, in contrast to graphene, BN is an insulator with large band gap and low dielectric constant, sharing with graphene high mechanical resistance.[4–6] Another distinctive property of BN sheets in comparison to graphene is its high thermal stability and chemical inertness.[7,8] Whereas graphene undergoes combustion upon heating the material in the presence of oxygen, sl-BN does not undergo combustion or chemical oxidation. The main application of sl-BN in electronics is to act as a nanometric barrier to prevent charge leakage.[9, 10] Another unique property of sl-BN is light emission in the deep UV region ($\lambda \leq 200$ nm).[11,12] To our knowledge, the catalytic properties of BN have, to date, not been reported.

Among the different preparation procedures for sl-BN films, the most important ones are chemical vapor deposition of aminoborane and other precursors on metal surfaces[8,11,13–17] or exfoliation of bulk h-BN particles.[18–23] Thin-walled bubbles of BN or C_xBN have been obtained by multistage heating of aminoborane in the absence or presence of ethanol.[24] However, compared to graphene, exfoliation of bulk h-BN particles is considerably inefficient, due to the reluctance of h-BN to undergo oxidation, which is the key step in the conversion of graphite into single-layer graphene oxide.[25] The mass of h-BN dispersed is negligible. Exfoliation of bulk BN in solvents such as DMF or *N*-methylpyrrolidone also results in a negligible dispersed mass. Therefore, it is highly desirable to develop alternative procedures for the preparation of single-layer or few-layers BN sheets, either as films or in suspension in water or low-viscosity solvents.

Herein, an innovative procedure for the synthesis of few-layers BN (fl-BN) sheets deposited on arbitrary substrates or suspended in conventional solvents is presented. Our procedure does not require specific equipment and is reliable, making sl-BN or fl-BN available for study. We found that the chemical inertness of fl-BN makes it a suitable and efficient catalyst for the Fenton-like degradation of pollutants.

Results and Discussion

The procedure reported herein can be applied to the preparation of nanometric fl-BN films or loosely crystallized h-BN powders that can be easily exfoliated by sonication. The process consists of the pyrolysis under inert atmosphere at temperatures above 900 °C of a homogeneous mixture of $(NH_4)_3BO_3$ and chitosan (Figure 1). Chitosan is a natural polysaccharide obtained from the skin of crustaceans and is the largest fisheries industry waste.[26] Pyrolysis under an inert atmosphere of chitosan, as single source of C and N, affords a turbostratic graphitic residue that can be easily exfoliated to form N-doped graphene (7 wt% N).[27–29] Herein, the ability of chitosan to form uniform films and embed inorganic compounds during pyrolysis has been used to template the formation of thin fl-BN films together with the graphitic carbon residue. The templating effect of chitosan is derived from a combination of features, including the ability of chitosan to embed $(NH_4)_3BO_3$ and still form films and, in the pyrolysis step, to segregate itself as graphene separate from the BN phase. Subsequently, combustion of the carbon material in air renders either fl-BN films or easily exfoliable BN powders. The merit of the present procedure is that, whereas highly crystalline BN powders do not undergo exfoliation upon sonication due to the close packing of

[a] Dr. A. Primo, Dr. S. Navalón, Prof. H. García
Instituto de Tecnología Química CSIC-UPV and Departamento de Química
Univ. Politécnica de Valencia, Av. de los Naranjos s/n
46022 Valencia (Spain)
E-mail: hgarcia@qim.upv.es

[b] Dr. A. M. Asiri, Prof. H. García
Center of Excellence for Advanced Materials Research
King Abdulaziz University, Jeddah (Saudi Arabia)

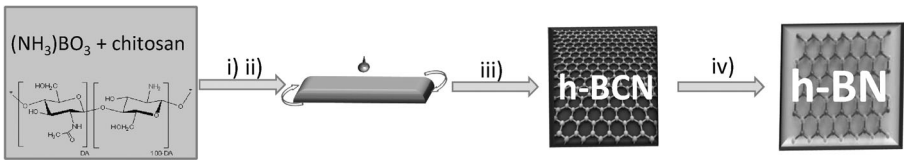

Figure 1. Preparation procedure for fl-BN films supported on arbitrary substrates. Steps i, iii and iv can be applied to obtain h-BN powders that can be easily exfoliated into few-layers BN platelets. i) Filtration of aqueous solutions; ii) spin coating; iii) pyrolysis at 900 °C under Ar; iv) calcination under air at 1000 °C.

the layers and the strong interaction between them, the present BN material from chitosan template undergoes a considerable degree of exfoliation upon sonication. This contrasting behavior is likely to be attributable to the poor crystallinity and loose packing of the BN material obtained in pyrolysis, allowing much easier deaggregation of the layers. Up to 50 wt% loadings of $(NH_4)_3BO_3$ vs. chitosan were achieved. Most of the experiments reported below were carried out with a $(NH_4)_3BO_3$ loading of 30 wt%.

Thermogravimetric analysis (TGA) of the samples after pyrolysis under argon containing C, B and N (sample after steps i–iii in Figure 1) was performed to determine the C vs. BN content. There was an initial weight loss from ambient temperature to 150 °C of about 6.4 wt% that we attribute to co-adsorbed water (Figure 2). After this weight loss, there was a plateau from 150 to 550 °C, indicating that the material is stable up to this temperature. From 550 °C up to 1000 °C there was a second weight loss of 13.8 wt%. This second weight loss was due to the combustion of residual carbon derived from chitosan present in the material. The high decomposition temperature is probably due to the effect of BN retarding the combustion of the carbon residue. According to this TGA, about 79.8 wt% of the material is stable at 1000 °C under air. This residual material is shown to have BN as chemical composition (see below).

BN films or powders resulting after pyrolysis under inert atmosphere and air calcination at 1000 °C were characterized by XRD, Raman spectroscopy, XPS, AFM, and electron microscopy. All data indicate the formation of highly crystalline BN films or powders.

XRD of h-BN is characterized by a (0002) reflection at 27°. Films of the material, resulting from pyrolysis of $(NH_4)_3BO_3$–chitosan mixtures and subsequent air calcination, supported on quartz also give rise to this characteristic peak on top of a broad background arising from the glass substrate. Figure 2 shows the XRD of a thick h-BN film (150 nm) on quartz showing the expected (0002) reflection. This diffraction peak was also observed for powders prepared according to Figure 1, except that spin coating (step ii) was replaced by lyophilization of the solution. Thinner films (50–150 nm) also showed this narrow peak, albeit with less intensity. However, for films of initial thickness below 50 nm before pyrolysis, the peak was barely distinguishable from the background or was completely obscured. This behavior is expected for very thin films in which the number of BN layers is small.

The same relationship between peak intensity and film thickness was shown by Raman spectroscopy. In contrast to graphene-based materials, which have relatively intense Raman bands, h-BN only gave rise to a sharp medium-intensity peak at about 1380 cm^{-1}. This expected vibration h-BN peak was detected for powders, but its intensity was too weak to be detectable for h-BN films of nanometric thickness. Figure 2 shows

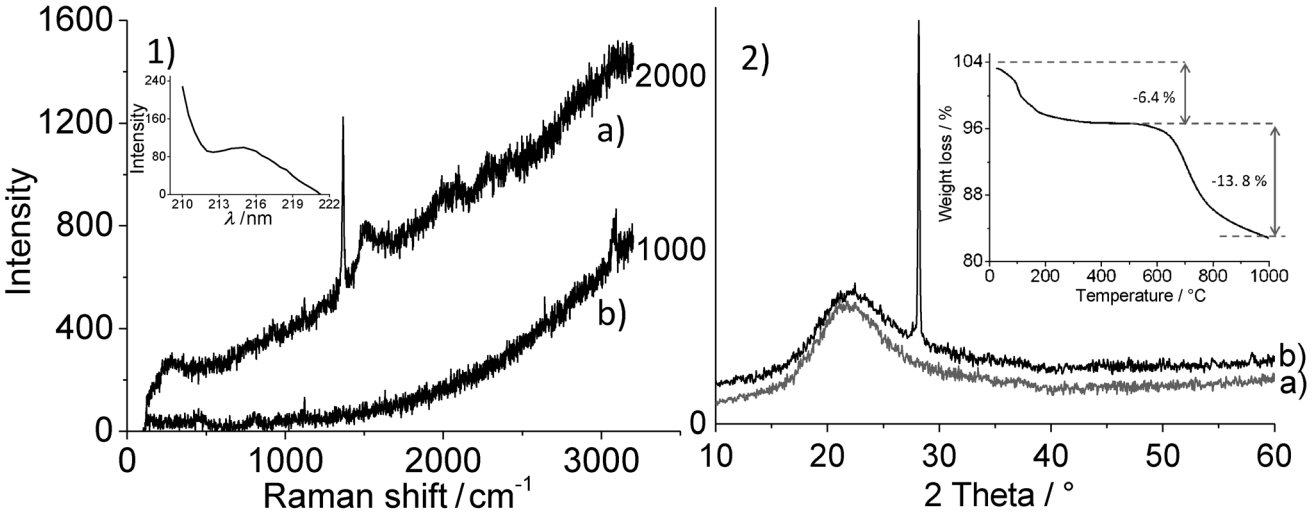

Figure 2. 1) Raman spectra of powders (a) and films on glass (b) of $(NH_4)_3BO_3$–chitosan mixtures after pyrolysis under Ar at 900 °C and subsequent air calcination at 1000 °C. The sharp peak at 1380 cm^{-1} has been reported as characteristic of BN. The inset shows the emission from BN powders having a $\lambda_{max} = 215$ nm upon excitation to 190 nm. This emission at such short wavelengths is due to the collapse by recombination of electrons and holes in high-quality BN materials; 2) XRD of a glass substrate submitted to pyrolysis at 900 °C under argon and subsequent air calcination at 1000 °C in the absence (a) or in the presence (b) of a thin h-BN film. The sharp peak appearing at 27° corresponds to h-BN. The inset shows the TGA profile of the residue after pyrolysis at 900 °C under inert atmosphere of a mixture of chitosan and ammonium borate (31 wt%).

the Raman spectra recorded for h-BN powders and films. Since single-layer graphene could be clearly detected by our Raman spectrophotometer, the absence of any peak for thin BN films indicates the total absence of carbon after air calcination.

XPS confirmed that, after calcination, both films and powders contained N and B with a 1:1 atomic ratio, detected at 398.2 and 190.75 eV, respectively (Figure 3). The B 1s peak shows a single component with binding energy coincident with that reported for B atoms in BN.[13] In the case of the N 1s peak, we observed two components, at an approximately 9:1 atomic ratio. For the more abundant component (90% of the total), the binding energy coincided with that reported for N atoms in BN.[13] The second N component (10% of the total) appeared at a lower binding energy (394 eV), attributable to N in the periphery and defects of the material. Accordingly, it is proposed that in our BN material, N is the element located at the periphery of the sheets.

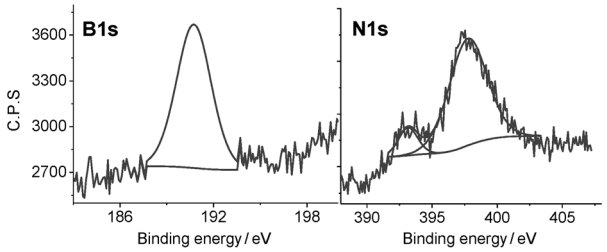

Figure 3. B 1s and N 1s XPS peaks recorded for BN films on glass obtained by pyrolysis at 900 °C under argon of $(NH_4)_3BO_3$–chitosan films and subsequent air calcination. Quantification of the intensity of the peaks indicates that the atomic B/N ratio is 1:1. The B 1s peak has a single component whose binding energy agrees with that reported for BN. In contrast, N 1s peak has two components in 90:10 ratio. The major one has a binding energy coincident to that reported for BN and the minor one is attributed to N atoms at the sheet periphery.

Our synthetic procedure for the preparation of BN films allows control of the film thickness by modifying the solution concentration and the spin coating rate. Chitosan forms high-quality nanometric films without defects and subnanometric roughness on arbitrary substrates, this being the key point to form single-layer or few-layers graphene on arbitrary substrates.[27] In the present case, the presence of $(NH_4)_3BO_3$ embedded in chitosan does not interfere with its ability to form this type of films. Upon pyrolysis and calcination of $(NH_4)_3BO_3$–chitosan films on quartz, optical microscopy showed smooth, highly cracked, transparent films. Prior studies on the formation of h-BN films on Ni substrates by chemical vapor deposition also reported a highly cracked film throughout the area covered by h-BN.[13] Figure 4 shows the optical microscopy image of BN films obtained by pyrolysis and calcination of $(NH_4)_3BO_3$–chitosan mixtures, which agrees well with reported images.[13]

The roughness and thickness of thin BN films on quartz were determined by AFM. Roughness values were measured by scanning the height variations of a $3\times3\ \mu m^2$ area and gave a value about 0.6 nm, agreeing with the expected BN single-layer thickness. Herein, the thickness of the resulting BN layer was varied from 200 to 20 nm by increasing the spin-coating velocity and maintaining the $(NH_4)_3BO_3$–chitosan concentration. As an example, Figure 4b shows the AFM image of a BN surface with a thickness of about 40 nm (the roughness was measured for a similar image). It should be noted, however, that the hardness of the BN film complicates these measurements since cuts on these surfaces are not easy.

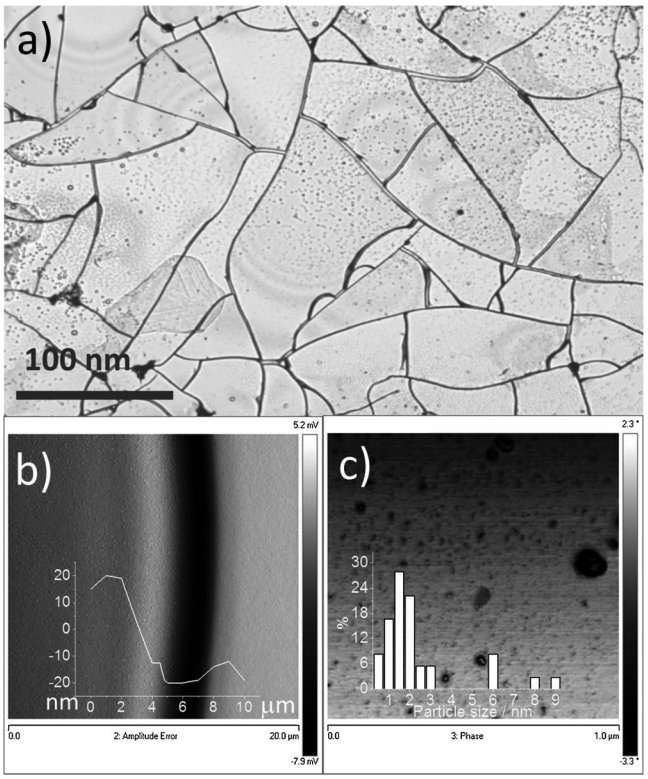

Figure 4. a) Optical microscopy image of a BN film on quartz obtained by pyrolysis of $(NH_4)_3BO_3$–chitosan at 900 °C under argon and subsequent calcination in air at 1000 °C. b) AFM image of a cut on the surface of a thin film of BN on quartz. The inset shows that the vertical height along the cut is about 40 nm. c) AFM image of BN platelets obtained by sonication of h-BN powders in water, showing dimensions ranging from 10 to 150 nm. The inset presents the statistical distribution of the height of these platelets showing that over 80% of the particles are constituted by fewer than four BN layers.

High-resolution transmission electron microscopy shows the crystallinity of the material, and, the single layer morphology can be observed at the borders. Selected-area electron diffraction shows intense spots indicating that the material is a single crystal with hexagonal arrangement at nanometric scale. In some parts, it has been possible to count the number of layers. As an example, Figure 5 shows an image of these crystals of 12 and 16 layers in two different particles (Figure 5a). A frontal view shows the material crystallinity (Figure 5b).

One of the properties that is characteristic of high-quality BN layers is deep UV emission.[11,12] Typically, organic materials emit in the UV or in the visible region, whereas materials having an emission below 220 nm are very scarce. BN is unique in this property. The BN samples obtained following the procedure described herein exhibited photoluminescence

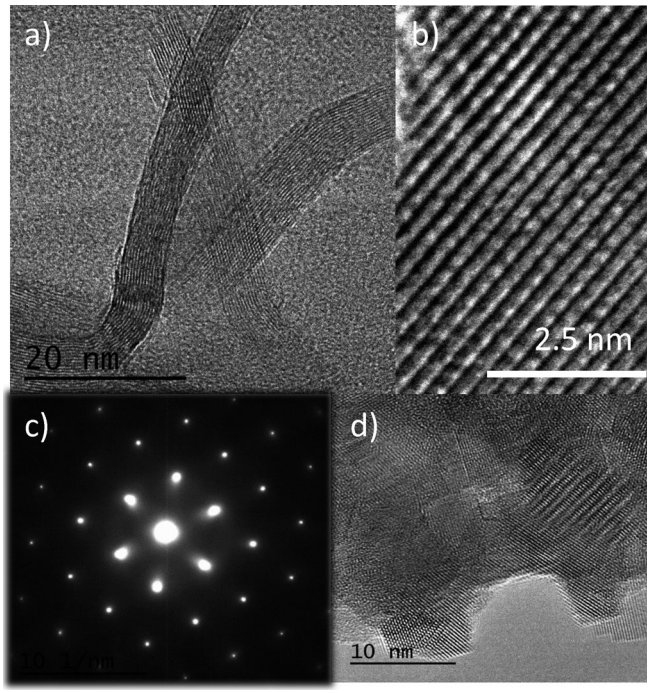

Figure 5. TEM images (a, b and d) of BN flakes after sonication in water. Panel (c) shows selected-area electron diffraction of the sample.

at 215 nm upon 190 nm excitation, this photoluminescence being distinctive of BN layers (inset of Figure 2.1).

To date, the unavailability of BN platelets has rendered study of their chemical properties impossible. In the present case, pyrolysis of $(NH_4)_3BO_3$–chitosan powders and subsequent air calcination led to particles whose XRD and Raman spectra (Figure 2) correspond to h-BN particles. Commercial h-BN powders cannot be exfoliated by sonication. In contrast, the loose stacking of h-BN particles obtained in the present case makes possible their dispersion upon sonication in water, ethanol, CH_2Cl_2, or other solvents, as revealed by dynamic laser scattering. AFM images of the BN platelets after sonication in water (Figure 4c) show that they are constituted by fl-BN particles of about 1.5 nm average height. The high degree of exfoliation explains why these fl-BN platelets form indefinitely persistent suspensions in water. To date, preparation of fl-BN suspensions in common solvents had proven difficult.

Having fl-BN suspensions in water, we considered the possibility that, due to its chemical stability, fl-BN could be a suitable catalyst to promote reactions in which highly aggressive chemical species are formed as reaction intermediates. Based on this hypothesis, and to show the potential of fl-BN as catalyst, we tested the activity of fl-BN to promote catalytic Fenton decomposition of H_2O_2 to generate hydroxyl radicals.[30] Hydroxyl radicals are the most aggressive chemical species known in aqueous media,[31] and are known to react with most organic compounds in water leading to their oxidative degradation up to the complete mineralization to CO_2 and inorganic salts. The Fenton reaction is typically carried out using stoichiometric amounts of iron(II) salts that cause O–O bond cleavage to give the hydroxide anion and hydroxyl radical [Eq. (1)]. There is an interest in developing catalytic systems for the Fenton reaction in where a site capable of transferring electrons to H_2O_2 initiates the Fenton reaction.[30] Subsequently, due to the intermediate O oxidation state in peroxides, H_2O_2 itself can reduce the oxidized catalytic site evolving O_2 in the process.

$$Fe^{2+} + H{-}O{-}O{-}H \rightarrow Fe^{3+} + \cdot OH + OH^- \quad (1)$$

We anticipated that the presence of π and π^* orbitals in BN, as well as N atoms at the periphery of the sheets and possible dangling bonds and defects, would promote this catalytic activity. To check this possibility, we selected the degradation of phenol as a test reaction and followed its disappearance by H_2O_2 oxidation in the presence and absence of fl-BN. This reaction is of interest for waste water treatment of nonbiodegradable pollutants. Figure 6 shows the temporal profiles of phenol disappearance and H_2O_2 consumption, showing that the Fenton reaction can be catalyzed by fl-BN platelets. Complete phenol disappearance (Figure 6A) with a H_2O_2 consumption of about 8 equivalents (Figure 6B) was achieved. Furthermore, the fl-BN catalyst was recovered by centrifugation and used in a second Fenton reaction, giving rise to coincident temporal profiles (Figure 6A and B, open circles), indicating that fl-BN is

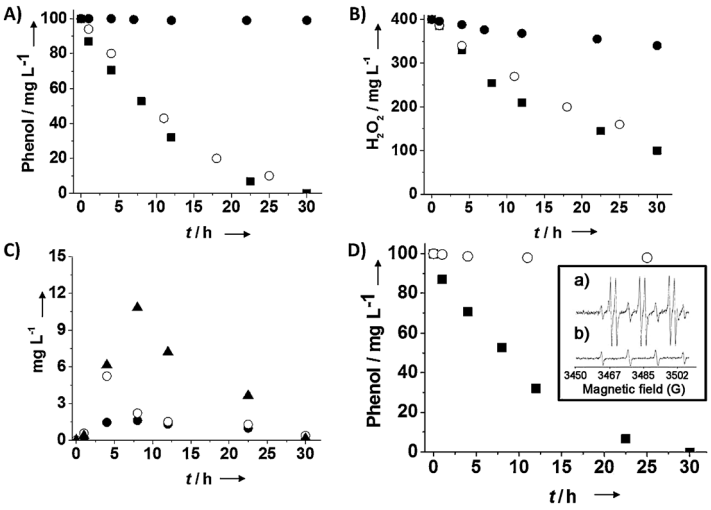

Figure 6. Phenol degradation (A) and H_2O_2 consumption (B) using fresh (■) and used (○) fl-BN or commercial BN (●) as catalyst. C) Product distribution as a function of time: hydroquinone (●), quinone (○), catechol (▲). D) Phenol degradation in the absence (■) or in the presence (○) of DMSO as hydroxyl radical scavenger. Reaction conditions: Catalyst (200 mg L^{-1}), phenol (100 mg L^{-1}), H_2O_2 (400 mg L^{-1}), DMSO/H_2O_2 molar ratio = 10:1, pH 3, room temperature. Inset. Experimental EPR spectra (black lines) of a) BN catalyst + H_2O_2 + PBNO at pH 3; Hyperfine coupling constants of PBNO–OH adduct: A_N = 15.5 G; A_H = 2.75 G, coinciding with reported values in the literature for the ·OH radical–PBNO adduct (red line).[39] b) BN catalyst + PBNO at pH 3. Hyperfine coupling constants from PBNO degradation A_N = 14.58 G; A_H = 13.90 G, coinciding with reported values in the literature for *tert*-butyl aminoxyl (red lines).[39] Conditions of the EPR measurements: BN catalyst (100 mg L^{-1}), H_2O_2 (200 mg L^{-1}), PBNO/H_2O_2 molar ratio = 1:1, pH 3, room temperature, 30 min reaction time.

not deactivated in the process. In an additional experiment to assess fl-BN catalytic stability, a 10 times-larger amount of phenol (1000 mg L^{-1}), close to the saturation limit at the reaction pH, was used alongside a 4 times-lower catalyst amount (50 mg L^{-1}), which effected complete phenol disappearance even under these conditions. Furthermore, H_2O_2 was not completely consumed (only 80%), maintaining the same 8 equivalent consumption as in the other experiments, indicating that there is not deactivation even under these conditions.

Most of the precedents in the catalytic Fenton degradation of phenol use a very large H_2O_2 excess, frequently above 1000 times.[31–34] In contrast, herein only 11 equivalents of H_2O_2 were employed but only 8 equivalents were consumed. This efficiency in the utilization of H_2O_2 is remarkable and close to the theoretical limit. Thus, oxidation of phenol to benzoquinone, via dihydroxybenzene intermediate, requires 3 equivalents of H_2O_2 [Eq. (2)], plus an additional 3 equivalents for site regeneration. Therefore, a total of 6 equivalents of H_2O_2 are necessary to catalytically convert phenol to benzoquinone, close to the 8 equivalents of H_2O_2 consumed in these experiments (Figure 6A and B). This is orders of magnitude more efficient that common Fenton catalysts reported. Therefore, the negligible H_2O_2 decomposition by fl-BN is very minor compared to previously reported catalysts.[31]

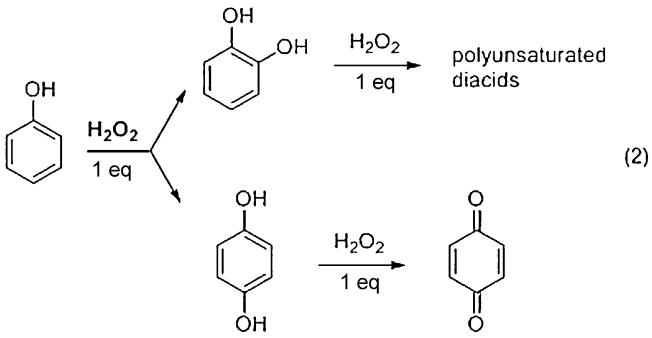

(2)

Analysis of the product distribution shows the formation of hydroquinone, catechol, and benzoquinone. The temporal evolution of these products (Figure 6C) shows that they are primary degradation products appearing since the initial reaction time, but that they undergo degradation over the course of the reaction, reaching concentration maxima and, then, their concentration diminishes at longer times. The high efficiency in the use of H_2O_2 and the low excess required for the complete disappearance of phenol using BN as catalyst can be understood considering that, once formed in the redox site, hydroxyl radicals will not have affinity for the surface of BN due to its chemical inertness and, therefore, they will become free ·OH radicals in solution. In most of the Fenton catalysts reported to date, ·OH radicals become attached to the metal and do not really form free ·OH radicals.[31] Only in a few cases, using extremely robust diamond nanoparticles, have ·OH radicals generated catalytically been claimed as free radicals in solution,[35] and the present case would be similar, considering that the surface of BN is even more inert.

To support the generation of free ·OH radicals, we carried out a test of phenol degradation in the presence of dimethyl sulfoxide (DMSO). DMSO is a known quencher of ·OH radicals.[36–38] DMSO acting as an ·OH quencher completely stops phenol degradation (Figure 6D). We also performed ·OH radical trapping using phenyl *tert*-butyl nitrone (PBNO) as quencher, monitoring the process by conventional EPR spectroscopy (Figure 6D, inset). As anticipated, the characteristic EPR spectra corresponding to the ·OH/PBNO adduct was recorded, providing firm evidence of the generation of free ·OH radicals by BN.

With respect to the nature of the active sites that reduce H_2O_2 to ·OH radicals, we propose that they could be N atoms at the periphery, probably bound to oxygen. To support this proposal, the catalytic activity of pyridine-*N*-oxide was checked. It was observed that this molecule was able to promote degradation of phenol, providing experimental evidence for the nature of the fl-BN active sites. Accordingly, the very low activity as a Fenton catalyst measured for commercial h-BN (Figure 6A and B, closed circles) compared to fl-BN should be due to the poor dispersibility in water of h-BN and the smaller population of active sites, rather than to structural differences between the two materials.

Conclusion

Herein, we have presented an innovative procedure based on the use of biomass waste to template the synthesis of fl-BN on arbitrary substrates or for fl-BN platelets in suspension. The success of the film formation derives from the known property of chitosan to form defect-free nanometric films with subnanometric roughness and its capability to embed ammonium borate, templating its pyrolysis. The pyrolysis of the $(NH_4)_3BO_3$–chitosan material led to the spontaneous segregation of BN and subsequent combustion of the carbon afforded fl-BN. The process can also be carried out with particles that, after easy exfoliation, formed fl-BN platelets suspended in water and other solvents. The quality of the BN materials was determined by electron microscopy and also by the characteristic deep UV photoluminescence. The BN platelets could be suspended in water, which allowed this material's activity as a Fenton catalyst to be tested, demonstrating an extremely high efficiency for the generation of free hydroxyl radicals without significant H_2O_2 decomposition.

Experimental Section

Synthesis of h-BN films

Prior to coating, the quartz supports were treated to increase their surface hydrophilicity. For this purpose, quartz plates (1×1 cm^2, 1 mm thick) were immersed overnight in a 1 M HCl aqueous solution and then washed exhaustively with Milli Q water, acetone, and isopropanol by sonication for 15 min in each solvent. After cleaning, the quartz plates were submitted to ozonization during 30 min to decompose any residual organic matter. Afterwards, an aqueous solution of chitosan (1.12 g, high quality chitosan of MW 60,000–120,000 from Aldrich, ref. 740063, dissolved in a 25 mL of 0.3 M acetic acid aqueous solution) and $(NH_4)_3BO_3$ (0.45 g) was

deposited on the freshly clean quartz support by spin coating (velocity varying from 2000 to 6000 rpm). The $(NH_4)_3BO_3$–chitosan film was pyrolyzed in an oven under argon flow (1 mL x min^{-1}) increasing the temperature at a rate of 0.9 °C min^{-1} up to 900 °C. Then, the pyrolyzed film was calcined in air up to 1000 °C, heating at a rate of 8 °C min^{-1}.

Exfoliation of h-BN crystals

h-BN powders were obtained by freeze-drying an aqueous solution of chitosan (1.12 g dissolved in 25 mL of 0.3 M HOAc) and $(NH_4)_3BO_3$ (0.45 g). The resulting $(NH_4)_3BO_3$–chitosan mixture was pyrolyzed under Ar flow at 900 °C and subsequently calcined in air at 1000 °C. Exfoliation was performed by suspending the h-BN powders in water and sonicating with an ultrasound horn (400 W) for 3 h. The resulting dispersion was left to stand for 24 h to allow any unstable aggregate to form and precipitate. At this time, the suspension was centrifuged for 30 min at 1500 rpm to obtain a homogeneous fl-BN dispersion that was indefinitely persistent.

Characterization techniques.

Raman spectra were recorded at ambient temperature with 514 nm excitation on a Renishaw In Via Raman spectrometer with a CCD detector. TEM images were recorded in a Philips CM300 FEG system with 100 kV operating voltage. XP spectra were recorded on a SPECS spectrometer with Phoibos 150 9 MCD detector using a non-monochromatic X-ray source (Al and Mg) operating at 200 W. The samples were evacuated in the prechamber at 1×10^{-9} mbar. The intensity ratios of components were obtained from the area of the corresponding peaks after nonlinear Shirley-type background subtraction and corrected by the transmission function of the spectrometer. X-ray diffraction patterns were obtained using a Philips X'Pert diffractometer and copper radiation ($Cu_{K\alpha}$; $\lambda = 1.541178$ Å). AFM measurements were conducted in contact mode in air at ambient temperature using a Veeco apparatus. AFM were not measured in a clean room and films on glass substrates may contain dust.

Catalytic tests

A Milli-Q water solution (100 mL) of phenol (100 mg L^{-1}, 1.06 mM) was placed in a round-bottom flask. fl-BN platelets or commercial h-BN catalyst (20 mg) were introduced and the suspension sonicated (400 W) for 3 h. Then, the initial pH was adjusted to 3 using HCl (0.1 M). Finally, H_2O_2 (400 mg L^{-1}, 30% v/v, 11.76 mM) was added. The reaction proceeded under ambient conditions. Once the reaction had finished, the catalyst was recovered by filtration (0.2 μm Nylon filter), washed with NaOH aqueous solution (pH 10; 20 mL), and with Milli-Q water (20 mL). Then, the solid was used for a second run. The productivity test was performed using a phenol solution (1,000 mg L^{-1}) containing the BN catalyst (50 mg L^{-1}), initial pH 3, and H_2O_2 as oxidant (4,000 mg L^{-1}) under ambient conditions.

Characterization of phenol degradation products

The organic products present in the aqueous solution were determined by reverse-phase chromatography using Kromasil-C18 column and a 69:30:1 (v/v/v) mixture of H_2O, MeOH, and CH_3COOH as eluent under isocratic conditions with a UV/Vis photodiode array detector. The monitoring wavelengths for phenol, hydroquinone, catechol, and quinone were 270, 290, 276, and 245 nm, respectively. Prior to analysis, aliquots of 2 mL were filtered through 0.2 μm Nylon filters. In the productivity test, 10-fold sample dilution was performed prior to analysis.

H_2O_2 measurements

H_2O_2 was determined by 40-fold (or 400-fold in the productivity test) dilution of the reaction mixture aliquots and using $K_2(TiO)(C_2O_4)_2$ in H_2SO_4/HNO_3 as colorimetric indicator. The indicator was prepared by dissolving the mixed potassium and titanyl oxalate (2.5 g) in concentrated sulfuric acid (2.5 g) and concentrated nitric acid (1 mL). After dissolution, the mixture was cautiously diluted with milliQ water to reach 100 ml indicator solution. The reaction was allowed to react for 10 min before monitoring at 420 nm in a UV/Vis spectrophotometer.

Quenching and EPR spin-trapping experiments

Hydroxyl radical scavenging was carried out using DMSO in the following conditions: Phenol (100 mg L^{-1}, 1.06 mM), H_2O_2 (400 mg L^{-1}, 11.76 mM), pH 3, catalyst (200 mg L^{-1}), DMSO/H_2O_2 molar ratio = 10:1, and 30 h reaction time. EPR spectra of PBNO and hydroxyl radical adduct were recorded using the following conditions: a) PBNO (100 mg L^{-1}), H_2O_2/PBNO molar ratio = 1:1, catalyst (200 mg L^{-1}), pH 3, 30 min reaction time; b) PBNO (100 mg L^{-1}), catalyst (200 mg L^{-1}), pH 3, 30 min reaction time. A Bruker EMX instrument was employed with the following settings: Frequency = 9.803 GHz, sweep width = 3489.9 G, time constant = 40.95 ms, modulation frequency = 100 kHz, modulation width 1 G, microwave power = 19.92 mW.

Acknowledgements

Financial support by the Spanish Ministry of Economy and Competitiveness (Severo Ochoa and CTQ2012–32315) is gratefully acknowledged. Generalidad Valenciana is also thanked for funding (Prometeo 2012/013 and GV/2013/040).

Keywords: boron nitride · heterogeneous catalysis · pyrolysis · template synthesis · UV emission

[1] T. P. Kaloni, Y. C. Cheng, U. Schwingenschlögl, *J. Mater. Chem.* **2012**, *22*, 919.
[2] O. Hod, *J. Chem. Theory Comput.* **2012**, *8*, 1360.
[3] D. Golberg, Y. Bando, Y. Huang, T. Terao, M. Mitome, C. Tang, C. Zhi, *ACS Nano* **2010**, *4*, 2979.
[4] J. Furthmüller, J. Hafner, G. Kresse, *Phys. Rev. B* **1994**, *50*, 15606.
[5] M. Pashangpour, Z. Bagheri, V. Ghaffari, *Eur. Phys. J. B* **2013**, *86*, 269.
[6] D. Lahiri, F. Rouzaud, T. Richard, A. K. Keshri, S. R. Bakshi, L. Kos, A. Agarwal, *Acta Biomater.* **2010**, *6*, 3524.
[7] Y. Lin, J. W. Connell, *Nanoscale* **2012**, *4*, 6908.
[8] C. Zhi, Y. Bando, C. Tang, H. Kuwahara, D. Golberg, *Adv. Mater.* **2009**, *21*, 2889.
[9] M. P. Levendorf, C. J. Kim, L. Brown, P. Y. Huang, R. W. Havener, D. A. Muller, J. Park, *Nature* **2012**, *488*, 627.
[10] G. Giovannetti, P. Khomyakov, G. Brocks, P. Kelly, J. V. D. Brink, *Phys. Rev. B* **2007**, *76*.
[11] J. Yu, L. Qin, Y. Hao, S. Kuang, X. Bai, Y. M. Chong, W. Zhang, E. Wang, *ACS Nano* **2010**, *4*, 414.
[12] K. Watanabe, T. Taniguchi, H. Kanda, *Nat. Mater.* **2004**, *3*, 404.
[13] Y. Shi, C. Hamsen, X. Jia, K. K. Kim, A. Reina, M. Hofmann, A. L. Hsu, K. Zhang, H. Li, Z. Y. Juang, M. S. Dresselhaus, L. J. Li, J. Kong, *Nano Lett.* **2010**, *10*, 4134.
[14] P. Sutter, J. Lahiri, P. Zahl, B. Wang, E. Sutter, *Nano Lett.* **2013**, *13*, 276.

[15] A. Ismach, H. Chou, D. A. Ferrer, Y. Wu, S. McDonnell, H. C. Floresca, A. Covacevich, C. Pope, R. Piner, M. J. Kim, R. M. Wallace, L. Colombo, R. S. Ruoff, *ACS Nano* **2012**, *6*, 6378.
[16] K. K. Kim, A. Hsu, X. Jia, S. M. Kim, Y. Shi, M. Dresselhaus, T. Palacios, J. Kong, *ACS Nano* **2012**, *6*, 8583.
[17] L. Song, L. Ci, H. Lu, P. B. Sorokin, C. Jin, J. Ni, A. G. Kvashnin, D. G. Kvashnin, J. Lou, B. I. Yakobson, P. M. Ajayan, *Nano Lett.* **2010**, *10*, 3209.
[18] G. Lian, X. Zhang, M. Tan, S. Zhang, D. Cui, Q. Wang, *J. Mater. Chem.* **2011**, *21*, 9201.
[19] Y. Lin, T. V. Williams, J. W. Connell, *J. Phys. Chem. Lett.* **2010**, *1*, 277.
[20] R. J. Smith, P. J. King, M. Lotya, C. Wirtz, U. Khan, S. De, A. O'Neill, G. S. Duesberg, J. C. Grunlan, G. Moriarty, J. Chen, J. Wang, A. I. Minett, V. Nicolosi, J. N. Coleman, *Adv. Mater.* **2011**, *23*, 3944.
[21] K. Sohaumburg, Vol. WO 2009047324 A2 20090416, 2009.
[22] Y. Wang, Z. Shi, J. Yin, *J. Mater. Chem.* **2011**, *21*, 11371.
[23] J. H. Warner, M. H. Rümmeli, A. Bachmatiuk, B. Büchner, *ACS Nano* **2010**, *4*, 1299.
[24] X. Wang, C. Zhi, L. Li, H. Zeng, C. Li, M. Mitome, D. Golberg, Y. Bando, *Adv. Mater.* **2011**, *23*, 4072.
[25] S. Stankovich, D. A. Dikin, R. D. Piner, K. A. Kohlhaas, A. Kleinhammes, Y. Jia, Y. Wu, S. T. Nguyen, R. S. Ruoff, *Carbon* **2007**, *45*, 1558.
[26] M. N. V. Ravi Kumar, *React. Funct. Polym.* **2000**, *46*, 1.
[27] A. Primo, P. Atienzar, E. Sanchez, J. M. Delgado, H. García, *Chem. Commun.* **2012**, *48*, 9254.
[28] M. Z. Elsabee, E. S. Abdou, *Mater. Sci. Eng. C* **2013**, *33*, 1819.
[29] A. Primo, E. Sánchez, J. M. Delgado, H. García, *Carbon* **2014**, *68*, 777.
[30] S. Navalon, M. de Miguel, R. Martin, M. Alvaro, H. García, *J. Am. Chem. Soc.* **2011**, *133*, 2218.
[31] S. Navalon, M. Alvaro, H. García, *Appl. Catal. B* **2010**, *99*, 1.
[32] S. Caudo, G. Centi, C. Genovese, S. Perathoner, *Appl. Catal. B* **2007**, *70*, 437.
[33] G. Centi, S. Perathoner, T. Torre, M. G. Verduna, *Catal. Today* **2000**, *55*, 61.
[34] S. Perathoner, G. Centi, *Top. Catal.* **2005**, *33*, 207.
[35] S. Navalon, R. Martin, M. Alvaro, H. García, *Angew. Chem.* **2010**, *122*, 8581; *Angew. Chem. Int. Ed.* **2010**, *49*, 8403.
[36] M. J. Burkitt, R. P. Mason, *Proc. Natl. Acad. Sci. USA* **1991**, *88*, 8440.
[37] S. Navalon, R. Martin, M. Alvaro, H. García, *ChemSusChem* **2011**, *4*, 650.
[38] S. Navalon, D. Sempere, M. Alvaro, H. García, *ACS Appl. Mater. Interfaces* **2013**, *5*, 7160.
[39] G. R. Buettner, *Free Radical Biol. Med.* **1987**, *3*, 259.

Received: September 30, 2014
Published online on ■■ ■■, 0000

FULL PAPER

Boron Nitride

A. Primo, S. Navalón, A. M. Asiri, H. García**

■■ – ■■

Chitosan-Templated Synthesis of Few-Layers Boron Nitride and its Unforeseen Activity as a Fenton Catalyst

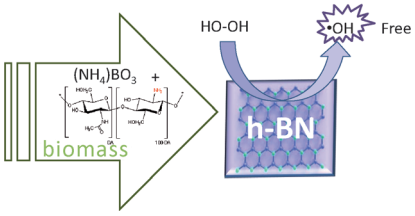

Ça va BN, merci: Few-layers boron nitride (BN) is synthesized, either as films or as suspended BN platelets, by pyrolysis of chitosan, which serves as a matrix to embed ammonium borate and as a template. The resulting samples exhibit deep UV emission characteristics of high quality BN. The few-layers BN is a highly efficient Fenton catalyst for the generation of hydroxyl radicals in water.